

Minimum number of azimuth sectors for seismic anisotropy estimation.

Peter Mesdag* and Leonardo Quevedo, CGG.

Summary

In this paper we present a practical extension of earlier work on the estimation of anisotropy parameters from isotropic techniques. We will take a closer look at the implications of working with effective elastic parameters in anisotropic (TI) seismic reflection inversion. In particular, for HTI media, the magnitude of the azimuthal Fourier terms is assessed. For many natural rocks the harmonic equations describing effective HTI anisotropy can be simplified, allowing for faster and more cost effective estimation of the magnitude and orientation of the anisotropy. Limits to these approximations in terms of the number of input azimuthal sectors used in the estimations are discussed.

Introduction

Mesdag and Quevedo (2017) outlined a method that allows the usage of isotropic modeling and inversion algorithms in an anisotropic setting. Based on the anisotropic Ruger reflectivity equations, they defined effective elastic parameters for VTI and HTI media. These effective elastic parameters can be used in the isotropic reflectivity equations to mimic the anisotropic character of the seismic reflectivity.

Quantitative measures of anisotropy and azimuth may be derived from azimuthally-sectored pre-stack inversions using Fourier analysis. Theoretically, for HTI anisotropy, there are three Fourier coefficients: a DC, a second and a fourth harmonic. The second and fourth harmonics are complex numbers, so it was stated that you need five or more azimuthal sectors to accurately capture the anisotropic character of the inverted elastic parameters.

Here we will show that, for many natural rock types, this requirement can be relaxed as the amplitude of the fourth harmonic is much smaller than the amplitude of the second one. So, once you have verified from wells or other anisotropic measurements that this is the case, you may reduce the number of azimuthal sectors to three and still get an accurate estimate of the anisotropy and the azimuth. Limiting the required number of azimuths to three can simplify the seismic acquisition and will reduce the amount of work and effort required during the processing and analysis of the data.

In this paper we discuss the character of the anisotropy that leads to a small fourth harmonic. Results from a synthetic

case will be shown using both six and three azimuthal sectors in the analysis. We will also show what happens if the assumption is not met, using an example where the fourth harmonic is significantly larger than the second.

Background

It can be shown (Mesdag, 2017) that, when taking the natural logarithm of the effective elastic parameters the azimuthal behavior for HTI media reduces to a Fourier series:

$$A' = b_0 + b_1 \cos[2(\phi - \omega)] + b_2 \cos[4(\phi - \omega)] \quad (1)$$

where A' is the logarithm of the inverted elastic parameter, b_0 , b_1 and b_2 are the amplitudes of the Fourier coefficients, ϕ is the azimuth of the anisotropy and ω is the azimuth of the seismic sector. Knowing the Thomsen parameters and the isotropic elastic parameters, the amplitudes of the Fourier coefficients can be calculated for any inverted elastic parameter set. Most seismic data lack the wide offset range or data quality threshold to accurately invert for density, so here we focus on the second inversion parameter and choose, for instance, V_p/V_s .

$$\begin{aligned} b_0 &= \ln \frac{V_p}{V_s} - \frac{1}{2} \ln \gamma_r^{(v)} + \left(\frac{4K+3}{64K} \right) \ln \delta_r^{(v)} + \left(\frac{12K-3}{64K} \right) \ln \varepsilon_r^{(v)} \\ b_1 &= -\frac{1}{2} \ln \gamma_r^{(v)} + \left(\frac{1}{16K} \right) \ln \delta_r^{(v)} + \left(\frac{4K-1}{16K} \right) \ln \varepsilon_r^{(v)} \\ b_2 &= -\left(\frac{4K-1}{64K} \right) \ln \delta_r^{(v)} + \left(\frac{4K-1}{64K} \right) \ln \varepsilon_r^{(v)} \end{aligned} \quad (2)$$

where $\varepsilon_r^{(v)}$, $\delta_r^{(v)}$ and $\gamma_r^{(v)}$ represent the Thomsen reflectivity parameters referenced to the isotropic plane of the HTI anisotropy and $K = (V_s/V_p)^2$. The Thomsen reflectivity parameters are defined as:

$$\varepsilon_r = \frac{\varepsilon+1-\bar{\varepsilon}}{1-\bar{\varepsilon}} \quad \delta_r = \frac{\delta+1-\bar{\delta}}{1-\bar{\delta}} \quad V_r = \frac{\gamma+1-\bar{\gamma}}{1-\bar{\gamma}} \quad (3)$$

where the overstrike above the parameter denotes an average (background) value.

Keeping in mind that in first order approximation for small values of x : $\ln(x_r) \approx x$, we can now simplify equations (2) to:

Minimum number of azimuth sectors

$$\begin{aligned}
 b_0 &= \ln \frac{V_p}{V_s} - \frac{1}{2} \gamma^{(v)} + \left(\frac{4K+3}{64K} \right) \delta^{(v)} + \left(\frac{12K-3}{64K} \right) \varepsilon^{(v)} \\
 b_1 &= -\frac{1}{2} \gamma^{(v)} + \left(\frac{1}{16K} \right) \delta^{(v)} + \left(\frac{4K-1}{16K} \right) \varepsilon^{(v)} \\
 b_2 &= -\left(\frac{4K-1}{64K} \right) \delta^{(v)} + \left(\frac{4K-1}{64K} \right) \varepsilon^{(v)}
 \end{aligned}
 \tag{4}$$

Note that there are two regimes for which the amplitude of the fourth harmonic vanishes.

The first case corresponds to elliptical HTI anisotropy, which is defined by the condition: $\delta \approx \varepsilon$.

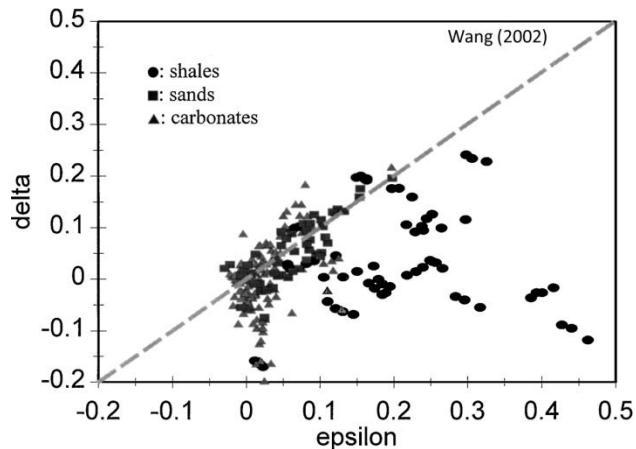


Figure 1: Anisotropic laboratory measurements on several rock cores

Wang (2002) published core data measurements, showing the values of the Thomsen parameters ε and δ . As can be seen in Figure 1, many measurements fall along the diagonal line in this crossplot, with most outliers being shales for which $\varepsilon > \delta$.

The second regime for which the fourth harmonic vanishes corresponds to the condition $V_p/V_s \approx 2$. In this case $K \approx 1/4$ and both terms of b_2 vanish. The condition of $V_p/V_s \approx 2$ is also not uncommon and has been used by several authors as a ‘typical value’ to derive simplified seismic relationships (see Whitcombe et al, 2002).

Though these conditions need to be verified by other measurements in and around well locations, it is reasonable to assume that in many cases, the amplitude of the first Fourier coefficient is much larger than the amplitude of the second Fourier coefficient: $b_1 \gg b_2$. In these cases the error

is small if we limit the Fourier expansion to only the first two coefficients of equation (1).

Azimuthal ambiguity of seismic reflectivity

It is well known that seismic reflectivity is ambiguous with respect to the azimuth of the anisotropy. For any model that explains the magnitude of the anisotropy with a certain azimuth there is also a model with opposite magnitude and a 90° azimuth shift. This behavior is encoded in the b_1 and b_2 of equation (4). The magnitude of these Fourier coefficients can be positive or negative.

Therefore, the post inversion analysis of the effective elastic parameters needs to be given prior information about the branch: is the b_1 expected to be positive or negative? Incorrect choice of this prior information will flip the azimuth by 90° .

Fortunately, for many natural rocks the positive branch may be chosen. If we assume elliptical anisotropy and substitute $\varepsilon = \delta$ for b_1 in equation (4), bearing in mind that for HTI media ε and γ are negative (higher velocities in the isotropic plane) we see that b_1 only becomes negative when the V_p anisotropy ε is more than twice the V_s anisotropy γ . Likewise, for $V_p/V_s = 2$ we see that b_1 only becomes negative when the magnitude of δ is more than twice γ .

Example

Here we will show an isotropic synthetic model containing three HTI layers with different characteristics. The isotropic models are combined with Thomsen parameters and the azimuth of the symmetry axis to derive azimuthally-varying effective elastic parameters for a six- and a three-azimuth sector case (Mesdag, 2017). From these effective elastic parameters the amplitude and phase of the azimuthal Fourier coefficients are determined. Figure 2 shows the process on a North-South and West-East section through the model. The arrows in the top panel of Figure 2 indicate where the three anisotropic layers are in the isotropic model.

In the first anisotropic layer the Thomsen parameters are chosen such, that the fourth harmonic of V_p/V_s (b_2) is zero and the second (b_1) varies between negative and positive values. In the second anisotropic layer $b_1 = 0$, while in the third anisotropic layer $b_1 > 0$ and $b_1 \gg b_2$. Keep in mind that in most natural rocks $b_1 > 0$ and $b_1 \gg b_2$, so the first and second anisotropic layer are hypothetical, and designed to test the analysis method.

Minimum number of azimuth sectors

The second anisotropic layer lies directly on top of the third anisotropic layer and only differs in the isotropic elastic parameters. The Thomsen parameters are the same for the two layers. Yet, the anisotropic behavior of these two layers is completely different. This shows that the anisotropic character of the seismic reflections is not only influenced by the inherent anisotropy, but it is also a function of the isotropic elastic parameters.

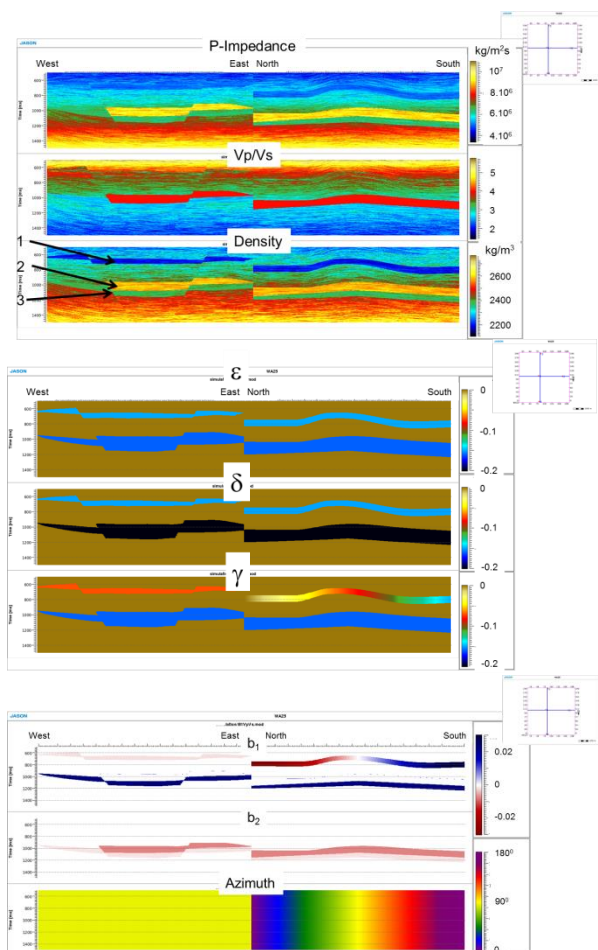


Figure 2: Cross sections through a model, depicting the isotropic elastic parameters (top), the Thomsen parameters (middle) and the calculated azimuthal Fourier coefficients b_1 and b_2 as well as the modeled azimuth of the HTI symmetry axis (bottom).

In the azimuthal analysis of the effective elastic parameters we are able to choose from three prior conditions. We can choose a positive or a negative branch for the Fourier coefficient b_1 , or we can enter a prior constraint on the anisotropy azimuth. Figure 3 shows the results of the analysis using each of these three conditions.

Figure 4 shows the Fourier analysis results for the case where we only use three azimuth sectors in the analysis, and we constrain the analysis by using a prior azimuth.

Comparing the anisotropy magnitude and azimuth in figures 2, 3 and 4 we can draw some interesting conclusions.

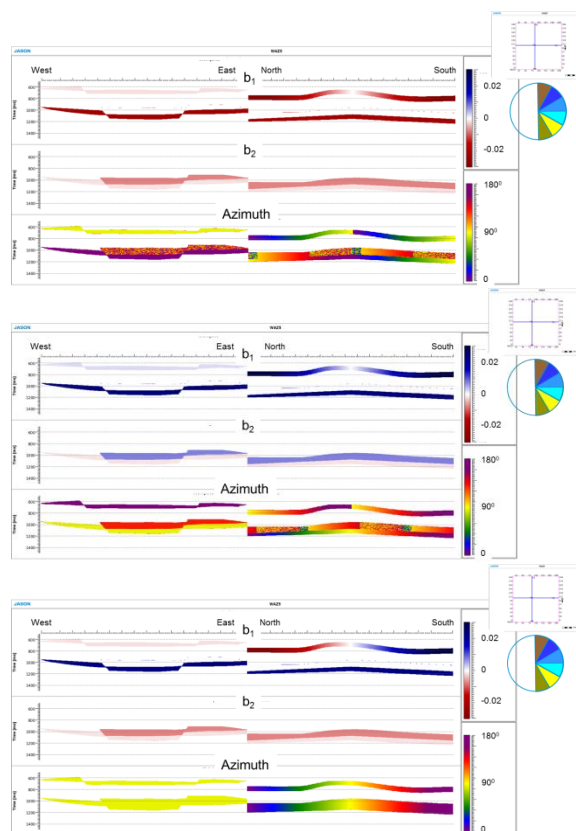


Figure 3: Results from azimuthal Fourier analysis. Top: negative branch; middle: positive branch; bottom: prior azimuth.

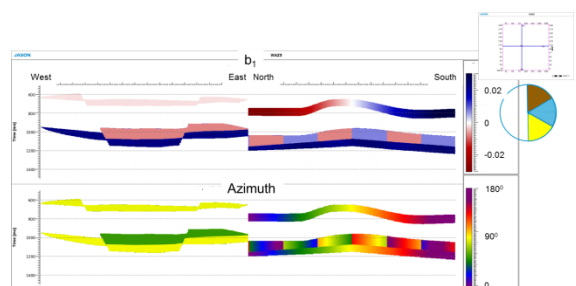


Figure 4: Fourier analysis using three azimuth sectors only.

In the first anisotropic layer, the choice of the branch in the Fourier analysis cannot be done correctly for the whole

Minimum number of azimuth sectors

model. To the North we need a negative branch and to the South a positive one. The top two panels in Figure 3 show that, if the branch is chosen incorrectly, the extracted anisotropy azimuth is rotated by 90° .

The second anisotropic layer, where $b_1 = 0$, shows a clear case where a three-azimuth analysis will fail while the six-azimuth analysis performs well if we are able to define a prior azimuth. The three-azimuth case shows azimuthal aliasing for this layer, as the azimuthal variation is under-sampled. Choosing a branch for b_1 is insufficient to resolve an ambiguity that stems from the underfitted fourth harmonic term.

For the third anisotropic layer, the analyses perform perfectly for a positive branch or a prior azimuth, as the conditions that $b_1 > 0$ and $b_1 \gg b_2$ are fulfilled everywhere.

Conclusions

The formulation of effective elastic parameters to describe the anisotropic behavior of seismic reflections is a powerful tool to predict the outcome of an anisotropic measurement.

In many natural rocks, the fourth Fourier mode can be omitted in the azimuthal analysis of pre-stack inversion results.

If evenly distributed, the necessary number of seismic azimuth sectors to be inverted and analyzed can often be reduced to three without significant loss of accuracy in the estimated anisotropy.

REFERENCES

- Mesdag, P. R., and L. Quevedo, 2017, Quantitative inversion of azimuthal anisotropy parameters from isotropic techniques: *The Leading Edge*, **36**, 916–923, <https://doi.org/10.1190/le36110916.1>.
- Wang, Z., 2002, Seismic anisotropy in sedimentary rocks — Part 2: Laboratory data: *Geophysics*, **67**, 1423–1440, <https://doi.org/10.1190/1.1512743>.
- Whitcombe, D. N., P. A. Connolly, R. L. Reagan, and T. C. Redshaw, 2002, Extended elastic impedance for fluid and lithology prediction: *Geophysics*, **67**, 63–67, <https://doi.org/10.1190/1.1451337>.